CC-1065 Bonding to Intracellular and Purified SV40 DNA: Site Specificity and Functional Effects†

Mary M. McHugh,‡ Jan M. Woynarowski,‡,§ Mark A. Mitchell,∥ Loretta S. Gawron,‡ Katherine L. Weiland,∥ and Terry A. Beerman*,‡

Department of Experimental Therapeutics, Roswell Park Cancer Institute, 666 Elm Street, Buffalo, New York 14263, and Medicinal Chemistry Research, Upjohn Laboratories, Kalamazoo, Michigan 49001-0199.

Received January 18, 1994; Revised Manuscript Received May 2, 1994⊛

ABSTRACT: CC-1065 is a minor-groove bonding agent capable of forming covalent adducts with the N-3 position of adenines within A-T-rich regions of duplex DNA. By examining the formation and location of CC-1065 adducts within the simian virus 40 (SV40) DNA molecule, the present study marks the first time that the precise sites of CC-1065 lesions have been identified at the level of eukaryotic genomic DNA. In naked DNA preparations, *r* values (moles of drug/mole of nucleotide base pair) ≥ 0.0015 effected, after thermal treatment, a measurable decrease in intact supercoiled form I, as well as increases in forms II and III, indicating that both single-strand and apparent double-strand damage had occurred. A similar pattern of damage was observed in SV40-infected cells, albeit at higher CC-1065 levels. The amount of CC-1065 required to produce a 50% loss in form I was >2-fold higher in infected cells ($r = 0.029$) than with purified DNA samples ($r = 0.013$). The appearance of double-strand damage at low drug levels suggested a high specificity of CC-1065 bonding to localized regions of the genome. The precise location of these CC-1065 adduction sites was examined by three methods: sequence analysis of the entire genome (GenBank), DNA polymerase termination assay of specific fragments of SV40, and restriction enzyme digestion analysis of the entire SV40 molecule. When sequence analysis of the entire genome was performed by examining both strands for the presence of the consensus CC-1065 binding sequence 5′-A/T-A/T-A/T-A/T-A*-3′ [Reynolds et al. (1985) *Biochemistry 24*, 6228–6247], 294 single-strand adduction sites were predicted, compared to 20 sites where CC-1065 should bond to both strands within a 30-base-pair window and at which, when heated, a double-strand break should occur. DNA polymerase termination assay of actual adduction sites was performed on restriction fragments of SV40 DNA pretreated with CC-1065 in infected cells or in purified supercoiled DNA preparations and selected on the basis of the sequence analysis (i.e., regions 2510–2730, 3701–3920, 4400–4659, 4020–4320, and 5163–65). In general, double-strand lesions were detected in similar regions of the genome by the DNA termination assay and by sequence analysis. When restriction enzyme digestion and the DNA polymerase termination assay were compared throughout the genome, nearly identical patterns of adduct formation were observed. Interestingly, similar alkylation patterns were observed with either naked or infected cell DNA. The sites predicted by sequence analysis and observed in infected cells or with purified supercoiled SV40 DNA were localized to specific functional regions of the genome associated with attachment of SV40 DNA to the matrix and with DNA replication and separation of daughter molecules, as well as with production of essential viral proteins. Functional effects of CC-1065 adduct formation in SV40 included a decrease in SV40 DNA accumulation. When cells were drug treated at 2 h postinfection and then further incubated until 40 h postinfection, 50% and 100% decreases in accumulation of SV40 DNA were observed at 2.5 and 10 nM CC-1065, respectively. The formation of nascent SV40 DNA intermediates also was reduced, but not completely eliminated, in the presence of the drug. Each of the intermediates was inhibited to a similar extent, suggesting that drug action affected an early stage of replication.

CC-1065 is a potent cytotoxic antitumor agent first isolated by the Upjohn Company in 1978 from *Streptomyces zelensis* (Hanka et al., 1978). This drug was shown to be moderately effective against several murine tumors *in vivo* as well as human cell lines in culture (Bhuyan et al., 1982). Unfortunately, CC-1065 could not be evaluated clinically because it caused delayed deaths in nontumored mice at therapeutic doses (McGovren et al., 1984). More recently, analogs of CC-1065 have been synthesized which retain antitumor activity without exhibiting delayed toxicity (Petzold et al., 1985; Warpehoski, 1986), and one of them, adozelesin, currently is undergoing clinical testing (Li et al., 1991). These agents are referred to as CPI drugs because of the characteristic presence of a DNA-reactive cyclopropylpyrroloindole moiety on at least one of the molecule's aromatic rings.

Despite the lack of therapeutic utility of CC-1065, much of our understanding of the mechanism of action of CPI drugs was obtained with this agent. CC-1065 consists of three minor-groove binding subunits with the reactive cyclopropylpyrroloindole moiety in subunit A (see Figure 1). The drug binds to the minor groove and its curved shape facilitates its association within this region of duplex DNA. The preferred drug binding site is an A-T-rich[1] 5-base-pair sequence with an absolute requirement for adenine at the 3′ end (Reynolds

† This study was supported in part by grants from the National Cancer Institute (CA 28495 and CA 16056).

* To whom correspondence should be addressed.

‡ Roswell Park Cancer Institute.

§ Present address: Institute for Drug Development, Cancer Therapy and Research Center, San Antonio, TX 78245.

∥ Upjohn Laboratories.

⊛ Abstract published in *Advance ACS Abstracts,* July 15, 1994.

0006-2960/94/0433-9158$04.50/0

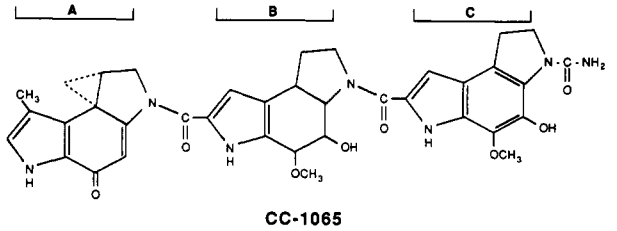

FIGURE 1: Structure of CC-1065.

et al., 1985). The reaction with DNA has been described as a multistep process where noncovalent interaction with the minor groove precedes covalent bonding reactions. Noncovalent binding to the minor groove occurs as a result of the interaction of all three subunits (Hurley et al., 1988). Studies with analogs of CC-1065 have attributed a significant portion of the noncovalent minor-groove affinity to the hydrophobic and van der Waals forces derived from the B and C subunits (Boger et al., 1990a; Hurley et al., 1988). The increased minor-groove affinity attributable to the B and C subunits provides for enhanced covalent reaction by CC-1065 and a significant increase in potency relative to the A subunit alone (Hurley et al., 1988). Formation of the CC-1065–DNA covalent adduct is essentially irreversible under physiological conditions (Warpehoski et al., 1992). Heating the DNA at 70 °C and above results in single-strand breaks at the site of adduct formation. Analyses of these strand breaks have been used to identify preferred sites of alkylation within DNA fragments (Reynolds et al., 1986).

While our knowledge of the interaction of the CPI moiety with DNA appeared extensive, it was unclear whether the sequence information obtained with purified DNA was valid for interpreting drug interactions with DNA as it existed in the eukaryotic cell. Indeed, other workers have reported that both noncovalent and covalent interactions of CC-1065 and chromatin from P388 cells were significantly reduced compared to interactions with naked DNA (Moy et al., 1989). In view of this study, the presence of chromatin and other cellular factors might well limit the sites available for drug–DNA binding and alkylation.

SV40 viral DNA provided a useful model for determining drug effects on higher order eukaryotic DNA structures. Since the sequence of the entire viral genome is available (GenBank), the identification of probable drug binding sites is possible when the base sequence preference of the drug is known. The functional regions of the SV40 molecule responsible for encoding the viral proteins and the start and stop sites for DNA replication (origin and terminus regions, respectively) have been defined (Tooze, 1980) and may be examined for site-specific damage induced by DNA reactive agents. Quantitative strand damage to the SV40 DNA molecule also may be readily measured. SV40 DNA is a circular supercoiled molecule of 5243 base pairs. Forms conversion analysis [reduction in the proportion of form I (supercoiled) and increases in forms II (nicked circular) and III (linear)] DNA provide simple quantitation of the extent of drug-induced DNA strand damage (Grimwade et al., 1986). A recent study in this laboratory showed that CC-1065 could induce heat-labile covalent DNA adducts in SV40-infected BSC-1 cells (Zsido et al., 1991). Approximately 10-fold more drug was required to induce single-strand damage to intracellular SV40 than to uninfected BSC-1 cell genomic DNA. The DNA strand damage observed correlated with cytotoxicity. CC-1065 was highly cytotoxic to BSC-1 cells, effecting a D_{10} (the dose effecting a 90% decrease in relative plating efficiency) at 0.5 nM concentration.

Given the feasibility of utilizing the BSC-1 cell/SV40 virus system for detection of CC-1065 adducts in eukaryotic cells, the present study examined the extent and localization of these lesions in naked and intracellular SV40 DNA. Structural damage to DNA was monitored by assaying the conversion of SV40 topological forms with increasing concentrations of CC-1065. The precise location of the lesions also was examined. In particular, we wished to address the question of whether CC-1065 showed the same bonding site specificity with intracellular SV40 DNA as has been reported for naked DNA. Examination of the entire SV40 genomic sequence for the existence of purported CC-1065 preferred binding sites, DNA polymerase termination assay of selected genomic fragments, and restriction enzyme digestion analysis of CC-1065-treated SV40 DNA all were employed to define whether certain areas of the genome showed specificity for CC-1065 bonding. Additionally, the functional effects of CC-1065 treatment on intracellular SV40 replication were examined. The results indicated that, except for a requirement for higher drug levels, the pattern of CC-1065 adduct formation in infected cells is nearly identical to that observed with the purified SV40 DNA molecule. This pattern is, in turn, very similar to that predicted by analysis of the SV40 genome for the presence of the CC-1065 consensus binding sequence. An important consequence of CC-1065 interaction with SV40 DNA is a significant alteration in viral replicative synthesis.

EXPERIMENTAL PROCEDURES

Chemicals. CC-1065 is produced by the Upjohn Co. (Kalamazoo, MI). Stock solutions in dimethylacetamide (Aldrich Chemical Co., Milwaukee, WI) were stored at −20 °C. SV40 DNA was purchased from Gibco-BRL (Grand Island, NY) and was diluted in sterile water just before use. [^{32}P]dCTP was obtained from Dupont-NEN (Boston, MA). [2-^{14}C]Thymidine (56 mCi/mmol) was purchased from Moravek Biochemical, Inc. (Brea, CA). T7 QuickPrime oligonucleotide labeling ket was from Pharmacia (Milwaukee, WI). Sequenase kit was from U.S. Biochemical Corp. (Cleveland, OH). *Eco*RI, *Bam*HI, *Taq*I, *Bgl*I, RNase A, and proteinase K were from Boehringer Mannheim (Indianapolis, IN). Hybond-N nylon membranes were from Amersham (Arlington Heights, IL). All other chemicals were of reagent grade.

Cell Culture and Viral Infection. Maintenance of BSC-1 (African green monkey kidney) cells in minimal essential medium (MEM-2) and infection with 5–15 plaque-forming units of SV40 virus/6×10^5 cells was as described elsewhere (Grimwade et al., 1987).

CC-1065 Treatment of SV40 DNA. Purified SV40 DNA (800 ng) was incubated at 37 °C with 0.5–500 nM CC-1065 ($r = 1.5 \times 10^{-4}$ to 0.15) in 0.4 mL (final volume) of TE buffer [10 mM Tris-HCl, pH 7.6, and 10 mM ethylenediaminetetraacetic acid (EDTA)]. Intracellular induction of CC-1065 damage to SV40 DNA was performed as follows: BSC-1 cells (6×10^5/35-mm plate) were infected as described above with SV40 virus. After 40 h, plates were rinsed once and further incubated for 30 min with fresh medium, prior to treatment with 0.5–20 μM CC-1065 ($r = 2.7 \times 10^{-2}$ to 1) in medium (1 mL total volume). Following the incubation, medium was removed, and cells were rinsed once with phosphate-buffered saline (PBS). Reactions with both purified and intracellular DNA routinely were terminated by adjusting samples to a final concentration of 1% sodium dodecyl sulfate (SDS). Proteinase K (50 μg/mL) was added to intracellular

[1] Abbreviations: A, adenine; T, thymine.

samples, which were digested for an additional 2 h. All DNA samples were then extracted with phenol/chloroform/isoamyl alcohol (25:24:1) to remove unbound CC-1065, precipitated with ethanol, resuspended in TE buffer, and heated at 70 °C for 2 h to induce strand damage. Under these conditions, maximum heat induction of DNA strand damage was obtained without significant loss of form I due to nonspecific nuclease activity (data not shown). To determine r values for CC-1065 treatment of infected cells, the total DNA content in lysed samples (i.e., the quantity of DNA actually exposed to the drug) prior to phenol extraction and heat induction of damage was determined as follows. Nonextracted samples were electrophoresed on a 1% agarose gel in Tris–acetate–EDTA buffer (TAE), pH 8.3, for 3 h at 3 V/cm. Following electrophoresis, 5 mL of 200 μg/mL RNase A was pipetted over the gel, which was then overlaid with plastic wrap and incubated overnight at 24 °C. Gels then were stained with 1 μg/mL ethidium bromide, and the DNA in the sample lanes was quantitated by comparing its fluorescence to that of a series of DNA standards electrophoresed on the same gel. By this method, the total DNA in a 35-mm dish of BSC-1 cells 40 h postinfection was determined to be 12 μg.

Forms Conversion Analysis and Restriction Enzyme Determination of CC-1065-Adducted Sites on SV40 DNA. At least three samples per CC-1065 concentration were analyzed for damage to both intracellular and naked SV40 DNA. Samples were prepared as described in the preceding paragraph. After heating, samples were divided into two aliquots. One aliquot was divided into four fractions, each of which was subjected to digestion by one single-cut restriction enzyme (either *Eco*RI, *Bam*HI, *Taq*I, or *Bgl*I). The other aliquot was not restricted. Both nonrestricted and restricted samples were electrophoresed on 1% agarose gels, which were blotted to nylon membranes. Membranes from gels containing nonrestricted samples were used to quantitate forms conversion and typically were hybridized to the *Eco*RI–*Bam*HI fragment of SV40 DNA. Membranes containing restricted samples were hybridized to either the *Taq*I–*Bgl*I (in the case of *Taq*I- or *Bgl*I-digested samples) or *Eco*RI–*Bam*HI (*Eco*RI- or *Bam*HI-digested samples) fragments of SV40 DNA. Each of these fragments was α-^{32}P-radiolabeled using the T7 QuickPrime oligonucleotide labeling kit. Blotting, hybridization, and autoradiography of the blots were performed as described elsewhere (Sambrook et al., 1989). Autoradiograms were scanned using a Molecular Dynamics densitometer with ImageQuant software (Molecular Dynamics, Sunnyvale, CA) to permit analysis of band density. Forms conversion was followed by determining the concentration of any one form calculated as a fraction of the sum of all three forms. In restricted samples, the length of DNA fragments (determined by comparison to sized marker fragments of SV40) was used to determine the distance of the CC-1065-induced break from the unique enzyme restriction site.

Prediction of CC-1065-Induced Double-Strand Lesions by Determining the Location of CC-1065 Adduction Sites on Opposite Strands. The location of CC-1065 single-strand adducts was determined either by analysis of the entire SV40 genomic sequence (GenBank) for the presence of the CC-1065 consensus binding sequence or by direct determination of intracellular adduction sites using the DNA polymerase termination assay. A double-stranded heat-labile site would correspond to two nonoverlapping adducts at a preferred binding site (5′-A/T-A/T-A/T-A/T-A*-3′) located on opposite DNA strands several base pairs apart (predictions assumed a distance not greater than 30 base pairs). To pinpoint regions with high intensity sites as well as those with clusters of lower intensity sites, the data were smoothed by calculating moving averages of hit probabilities at each nucleotide position averaged over a window of ±10 base pairs:

$$D(N_i) = \frac{\sum_{i-w}^{i+w} I(N)}{2w+1} \quad (1)$$

where $D(N_i)$ is the moving average (hit density) at nucleotide N_i, $I(N)$ is the hit probability, and w is the window size (w = 10 base pairs).

DNA Polymerase Termination Assay of Selected CC-1065-Adducted SV40 DNA Fragments. CC-1065-treated SV40 DNA was prepared as described above except that heating at 70 °C to induce strand damage was not performed. The amount of DNA from treatment of intracellular or purified SV40 used for the sequencing reaction was 0.4 and 1.0 μg, respectively. Regions of interest for the DNA polymerase termination assay were determined by examining the genomic base pair sequence of SV40 (GenBank) for the presence of the consensus CC-1065 bonding sequence. Fragments assayed included 4410–4640, 3700–3920, 2560–2680, 5160–65, and 4050–4295. Oligonucleotides which flank these regions were synthesized for use as primers in sequencing the DNA by the dideoxynucleotide chain termination method (Sanger et al., 1977). DNA polymerase termination site analysis was performed as previously described (Weiland & Dooley, 1991). The termination sites were visualized by autoradiography of the nascent strand, while the alkylation event being evaluated occurred on the opposite, template strand.

Accumulation of SV40 DNA in CC-1065-Treated Virus-Infected Cells. Infection with SV40 virus was performed as described above except that BSC-1 cells were plated in 24-well dishes. Two hours after viral infection, medium was replaced with 1 mL of MEM-2 containing CC-1065 at the indicated concentrations. After 4 h at 37 °C, drug-containing medium was replaced with 1 mL of drug-free MEM-2 and the incubation was continued for an additional 36 h. The wells were rinsed with PBS and the cells were suspended in 0.2 mL of 1% SDS/well. After 2 h at 45 °C, proteinase K (0.1 mg/mL) was added and incubation continued for 4 h at 45 °C. Aliquots of lysates (40 μL) were electrophoresed on a 1% agarose gel in TAE buffer for 17 h at 0.7 V/cm. Gels were stained with ethidium bromide and photographed on an ultraviolet transilluminator with a Polaroid CU-5 land camera. The amounts of SV40 DNA in each lane were quantitated by scanning the negatives as described above for autoradiograms.

CC-1065 Effects on Nascent SV40 DNA. Changes in nascent SV40 DNA synthesized after CC-1065 treatment were quantitated as described elsewhere (Snapka et al., 1988) with some modifications. BSC-1 cells plated in 35-mm dishes were infected with 5–15 plaque-forming units of SV40 virus. Forty hours after infection, MEM-2 containing CC-1065 was added (1 mL final volume) and incubation was continued. After 2 h, drug medium was aspirated and the cells were further incubated with 0.25 mL of MEM-2 containing [^{14}C]-thymidine (2 μCi/mL) for 15 min at 37 °C. DNA replication was terminated by addition of 3 mL of 50 μM nonradioactive thymidine in PBS. After three more rinses with thymidine-supplemented PBS, the cells were scraped, diluted into 10 mL of PBS, and centrifuged for 5 min at 600 rpm. The pelleted cells were resuspended in lysing solution and incubated as described in the preceding paragraph. The incubated lysates were extracted with an equal volume of chloroform/isoamyl alcohol (24:1), and the DNA was recovered by ethanol

precipitation. Samples were dissolved in 40 μL of TE buffer. Agarose gel electrophoresis, ethidium bromide staining, and photography were as described above, except that samples were electrophoresed for 35 h. The gel was dried onto filter paper and loaded into a phosphorimager cassette (Molecular Dynamics, San Jose, CA) for 2 months before analysis using a Molecular Dynamics phosphorimager.

RESULTS

This study compared intracellular bonding by CC-1065 with that which would be predicted from the known CC-1065 consensus binding sequence. SV40 forms conversion was utilized to identify the drug concentrations necessary to produce equivalent damage to intracellular and purified DNA. These drug concentrations were used to determine site-specific damage within several small fragments of the genome (by means of the DNA polymerase termination assay) as well as throughout the entire genome (by restriction enzyme digestion analysis). The bonding sites obtained *in vivo* were contrasted with those which would have been predicted from analysis of the nucleotide base sequence of SV40 DNA (GenBank).

SV40 Forms Conversion Analysis of Heat-Induced CC-1065 Lesions. CC-1065 was shown elsewhere to bind and alkylate single strands of duplex DNA (Reynolds et al., 1986). Heating of this alkylated DNA at ≥70 °C resulted in a single-strand break at the drug bonding site. Since it provides a common DNA target in both a cell-free and intracellular environment, SV40 DNA was chosen as a model system to monitor the formation of these CC-1065-induced DNA lesions. Strand damage to SV40 is readily measurable. Drug-induced strand breaks on circular supercoiled SV40 DNA are determined by forms conversion analysis (Grimwade et al., 1987), visualized by electrophoresis on agarose gels. Conversion of form I (uncut supercoiled) to form II (nicked circular) requires at least one strand break per duplex molecule. At least two cuts per molecule are required for a double-strand break, resulting in formation of form III (linear) DNA. Because alkylation by CC-1065 is virtually irreversible under physiological conditions (Warpehoski et al., 1992), the extent of the strand damage observed should depend on the number of drug molecules available per unit of DNA, rather than on the absolute molarity of the drug solution. For this reason, the drug concentrations throughout this study are expressed as *r* values (moles of drug/moles of nucleotide base pairs). An earlier study from this laboratory showed that unbound drug present during heat induction of strand breaks contributed significantly to the DNA damage observed (Zsido et al., 1991). This damage was reduced, but not eliminated, by briefly washing cells in ethanol at the end of drug treatment. Because of our concern that ethanol might not effectively remove intracellular drug that was sequestered noncovalently in the minor groove, we utilized an alternate procedure in this study. Using purified DNA, it was found that addition of SDS to the CC-1065–DNA reaction followed by phenol extraction effectively prevented further alkylation occurring during heat induction of strand breaks. Intracellular damage was assayed in a similar fashion. After incubating for 2 h with CC-1065, cells were rinsed once with PBS and adjusted to 1% (final concentration) SDS. Proteinase K (50 μg/mL) was added and samples were digested for 2 h, extracted with phenol, and heated to induce strand damage. With this procedure, no more than 5% of the alkylation activity originally present in the medium remained associated with the cells after washing with PBS and lysing with SDS (data not shown). Thus, termination of the CC-1065 reaction with SDS and extraction of unbound drug with phenol was used routinely throughout the present study.

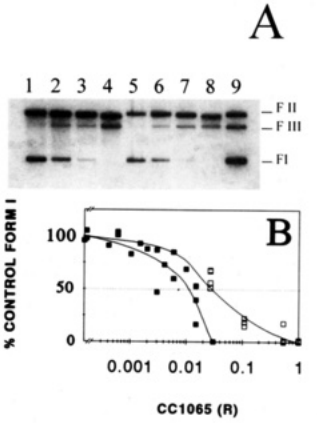

FIGURE 2: CC-1065 damage to purified and infected BSC-1 cell SV40 DNA: Forms conversion. Purified SV40 DNA and SV40-infected BSC-1 cells were treated with CC-1065 as described in Experimental Procedures. After thermally labile CC-1065 strand damage was induced by heating for 2 h at 70 °C, samples were subjected to agarose gel electrophoresis followed by Southern blotting and hybridization to an *Eco*RI–*Bam*HI fragment of SV40 DNA. Panel A: Representative agarose gel showing heat-induced forms conversion with increasing CC-1065. Lanes 1–4 are purified SV40 DNA treated with CC-1065 at *r* values of (1) 0, (2) 0.015, (3) 0.03, and (4) 0.15 (0, 50, 100, and 500 nM, respectively). Lanes 5–8 show SV40 DNA from infected BSC-1 cells treated with CC-1065 at *r* values of (5) 0, (6) 0.027, (7) 0.109, and (8) 0.546 (0, 0.5, 2, and 10 μM, respectively). Lane 9 is a representative SV40 DNA sample containing forms (F) I, II, and III. Panel B: Graphic analysis. Purified (■) or intracellular SV40 DNA (□) was treated with CC-1065 as described above. The data were expressed as a percent of the form I present in control (non-drug-treated) samples. Each point represents a minimum of 3 experiments.

Concentration-dependent effects on heat-induced changes in SV40 forms when either purified DNA preparations or infected cells were treated with CC-1065 are shown in Figure 2. Incubation of purified SV40 DNA with CC-1065 produced maximal decreases in form I within 15 min, while a 2-h incubation was necessary for infected cells (data not shown). The drug concentrations used *in vivo* and *in vitro* were those which effected decreases in form I from 0 to 100%. Panel A is a representative agarose gel showing SV40 DNA forms conversion with increasing levels of CC-1065. In purified DNA preparations, a pronounced decrease in intact supercoiled form I was observed with *r* values from 0.015 to 0.15 (0.5–500 nM) (lanes 2–4). Even at the lowest concentration, this decrease in form I was accompanied by an increase in both forms II and III, suggesting that both single- and double-strand damage had occurred. Accumulation of form III should result if two single-strand CC-1065 adducts were located in close proximity on opposite strands. Lanes 6–8 showed a similar pattern of damage to SV40 in infected cells, albeit at higher CC-1065 levels [$r = 0.027$–0.55 (0.5–10 μM)]. Panel B is a graphic representation of several experiments, performed as in panel A, showing that adduct formation by CC-1065 results, after thermal treatment, in a decrease in supercoiled form I. In this analysis, the amount of CC-1065 required to effect a 50% loss in form I was >2-fold higher in infected cells ($r = 0.029$) than with purified DNA samples ($r = 0.013$). Similarly, total disappearance of the form I band required a higher drug/DNA ratio for infected cells ($r \geq 0.55$) than purified SV40 DNA ($r \geq 0.15$). The rate of accumulation of forms II and III paralleled the decrease in form I shown in panel B (data not shown). At a given decrease in form I, the ratios of form III to form II were similar for treatment of either intracellular or purified DNA. These results indicated that the tendency of CC-1065 to bond to opposite strands at neighboring sequences did not depend on the source of the DNA at the time of treatment.

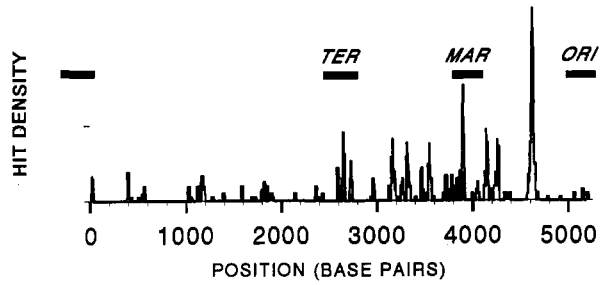

FIGURE 3: Sites of CC-1065-induced double-strand lesions in SV40 DNA predicted from examination of the entire 5243-base-pair genome (GenBank). A double-stranded heat-labile site was predicted when bonding by two nonoverlapping adducts occurred at a preferred binding site (5′-A/T-A/T-A/T-A*-3′) on opposite DNA strands no more than 30 base pairs apart. Data were plotted as described in Experimental Procedures. Labels on the figure refer to specific functional regions of the genome: (ORI) origin (Borowiec et al., 1990) and (TER) termination (Tooze, 1980), regions of viral replication, respectively; (MAR) nuclear matrix-associated region (Pommier et al., 1990).

Examination of the SV40 Genome for the CC-1065 Consensus Bonding Sequence. Forms conversion analysis provides a quantitative measure of drug lesions rather than specific information on the location of CC-1065 adduction sites. Since the entire base pair sequence of SV40 DNA, as well as the preferred sequence for CC-1065 binding, is known, it should be possible to identify probable drug bonding sites on the SV40 genome which would promote the formation of either a single- or double-strand lesion induced by CC-1065. We were particularly intrigued by the fact that double-strand damage (as evidenced by formation of form III) appeared at relatively low drug levels, and we wished to examine these potential "hot spots" for opposite-strand adduct formation.

Examination of the entire SV40 genome for the location of the binding sequence 5′-A/T-A/T-A/T-A/T-A*-3′ [2] revealed numerous potential sites on both strands (294 total) where single-strand adducts should occur (data not shown). To define whether CC-1065 bonding was targeted to any particular region(s) of the genome, the likelihood of a double-strand break occurring at any one nucleotide base pair was determined. For the analysis, we assumed that double-strand breaks were likely to occur when two nonoverlapping binding sites were located on opposite DNA strands over a distance not greater than 30 base pairs.[3] Figure 3 is a histogram showing probable double-strand break sites obtained by analysis of the entire 5243-base-pair sequence of SV40 DNA. To pinpoint regions with a high probability for forming double-strand lesions after treatment with CC-1065, as well as clusters of lower probability, the results were plotted as a function of hit density as described in the figure legend. It was readily apparent from inspection of the histogram that numerous regions existed where the formation of CC-1065-induced double-strand lesions could be predicted. Additionally, these sites were not evenly distributed throughout the genome. While several sites of lower intensity were located between 0 (origin) and 2500 base pairs, a much greater proportion of the appropriate binding sequences occurred between 2500 and 5243. The predicted formation of double-strand heat-labile sites was greatest at 4624–4625, compared to 3900–3903 and 2597–2599, where the probability was reduced by roughly half.

DNA Polymerase Termination Assay of Selected CC-1065-Adducted SV40 DNA Fragments. All the information on the preferred CC-1065 bonding sequence was obtained from earlier studies using purified DNA fragments. How drug bonding in these studies related to adduct formation in intracellular or purified genomic SV40 DNA remained to be determined. Differences due to the greater sequence diversity of the relatively large sized (5243 base pairs) SV40 DNA molecule, as well as protein association, might be expected to modulate CC-1065 interaction with its binding site. To explore this question, selected regions of the SV40 genome were examined by a DNA polymerase termination assay for the sequences at which covalent CC-1065 adducts are formed. This analysis was performed as described in Experimental Procedures. Briefly, CC-1065-treated SV40 DNA was prepared as described except that heating at 70 °C to induce strand breaks was not performed. Assay of CC-1065 adduction sites involved sequencing drug-treated DNA by the dideoxynucleotide chain termination method, which synthesized a nascent strand from the primed template. Electrophoresis of primer extension products from drug-treated DNA revealed sites of polymerase inhibition after autoradiography. In reactions where drug-treated DNA was used, discrete bands, indicating premature chain termination, were present that were not present in samples of untreated DNA. The CC-1065 alkylation sites were interpreted to be at the base adjacent to the termination site on the opposite (template) strand. Fragments of interest chosen for the DNA polymerase termination assay included regions identified by sequence analysis where binding would be expected to be greatest: 4410–4640, 3700–3920, and 2560–2680. In addition, fragments with a lower probability of adduct formation, 5160–65 and 4050–4295, were examined because of the functional importance of their locations within the origin and MAR (nuclear matrix-associated region) regions of SV40, respectively. The results of this analysis for the region 4050–4295 are shown in Figure 4. Panel A shows sequence ladders generated by CC-1065 treatment of intracellular or purified SV40 DNA. Strong termination sites (indicated by darker bands) were observed with naked DNA at $r = 0.0015$ and 0.015 (sets 3 and 4, respectively). At $r = 0.015$, naked DNA termination sites and readthrough were comparable to those for cellular SV40 reactions treated with $r = 0.273$ (set 4 compared to set 2). Interestingly, the precise sites and their relative intensities were nearly identical for sets 2 and 4, indicating nearly identical alkylation site specificity of this fragment for both intracellular and naked DNA treatments. Thus, the polymerase chain termination assay revealed little effect of the cellular "milieu" on CC-1065 adduct formation. Analysis performed on SV40 DNA isolated from cells treated with low doses of CC-1065 ($r = 0.054$) revealed no differences in the sites of alkylation when compared to samples treated with higher concentrations of CC-1065 ($r = 0.273$) (data not shown). The drug concentrations analyzed by the DNA termination assay of CC-1065 adducts in infected cell ($r = 0.054$) and purified SV40 DNA ($r = 0.015$) were found in Figure 2 to effect equivalent decreases (about 60%) in form I.

Panel B represents information from bidirectional sequence analysis of the region shown in panel A isolated from infected cells treated with CC-1065 ($r = 0.273$). Numerous sites of CC-1065 adduct formation were observed on both strands of this fragment, most being localized between 4100 and 4300 base pairs. The majority of CC-1065 alkylations were observed at adenines in 5′-ATA, TTA, or poly-A sequences. In contrast

[2] The preferred binding site was defined as 5′-A/T-A/T-A/T-A/T-A*-3′, on the basis of the consensus sequence reported elsewhere for preferred binding to runs of A-T base pairs (Hurley et al., 1990; Boger et al., 1991a).

[3] Because CC-1065-adducted DNA was heated at 70 °C to induce breaks, single-strand breaks on opposite strands separated by 30 base pairs would be expected to result in a double-strand break (Freifelder, 1969).

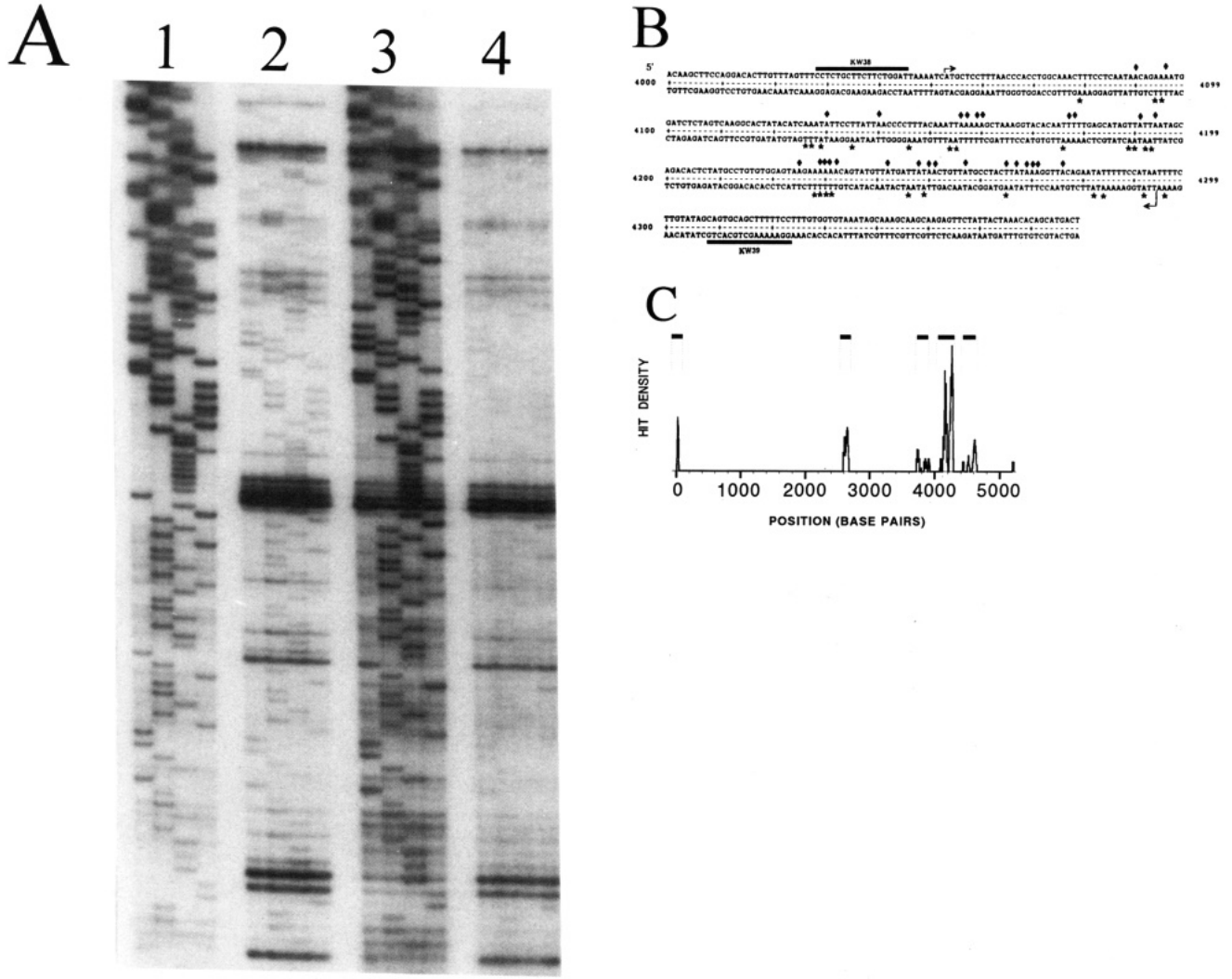

FIGURE 4: DNA polymerase chain termination sites in CC-1065-treated intracellular and purified SV40 DNA. Intracellular and purified SV40 DNA was treated with CC-1065 as described in Experimental Procedures except that adducts were not heated at 70 °C to induce strand breaks. Sequencing reactions were performed by the dideoxynucleotide chain termination method (Sanger et al., 1977). Panel A: Representative autoradiogram from the sequencing gel of region 4020–4294 of the SV40 genome. Sets 1 and 2 show the effect on intracellular SV40 DNA of CC-1065 treatment at r values of (1) 0 and (2) 0.273 (0 and 5 μM, respectively), while sets 3 and 4 show purified SV40 DNA treated with CC-1065 at r values of (3) 0.0015 and (4) 0.015 (5 and 50 nM, respectively). Individual lanes within each set correspond from left to right to G, A, T, and C sequencing lanes, respectively. Panel B: Intracellular SV40 DNA adduction sites of CC-1065 over the region 4050–4295. The double-stranded sequence of this region of SV40 is presented. KW38 and KW39, oligonucleotides which flank this region, were used as primers in sequencing DNA. The regions of DNA where primers anneal are highlighted by bars. For each primer, the readable sequence of the nascent strand starts at the arrow and proceeds in the direction of the arrow. The symbols ♦ and ★ denote the alkylated base on the template strand, which is judged to be one base in the 5′ direction on the opposite strand from the observed termination site. Panel C: Use of the DNA polymerase termination assay data to predict the location of CC-1065-induced double-stranded heat labile lesions on five regions of the SV40 genome (2500–2700, 3500–4000, 4050–4270, 4400–4650, and 5000–100) indicated by solid horizontal bars at the top of the figure. Positions of predicted double-strand adducts were defined, and data were plotted as described in Experimental Procedures.

to the findings reported earlier for the structurally simplified analog, adozelesin (Weiland & Dooley, 1991), CC-1065 termination sites sometimes appeared at non-adenine bases, usually thymine. These thymine termination sites were included in Figure 4B for completeness, but they probably represent overstabilization of the duplex and inhibition of polymerase passage regardless of whether the adenine alkylation occurs in the template or the polymerase displaced strand. In this work, these non-adenine termination sites were observed in long AT-containing stretches (e.g., 4093, 4094, 4127, 4128, 4228–4231, etc.) and occurred in regions where an adenine stop site was present nearby on the opposite strand.

Data obtained from experiments analogous to that described in Figure 4, panels A and B, were used to calculate the probable regions for localization of neighboring adducts on opposite strands. The probability of a double-strand heat-labile site occurring at a particular region of the fragments analyzed is shown in Figure 4, panel C. Since no difference was observed in sites of individual adduct formation when infected cells were compared to DNA, only data derived from infected cell studies are presented. Panel C shows the pattern of probable double-strand adduct formation in intracellular SV40 DNA treated with CC-1065 at $r = 0.273$ over the five regions of SV40 DNA subjected to the DNA polymerase termination assay. In general, double-strand lesion formation was predicted in the same regions determined by the DNA polymerase termination assay as were identified by examination of the known sequence of SV40 DNA (see Figure 3). While the relative density of formation of the adducts differed somewhat, these discrepancies may reflect ambiguity in the use of a "consensus" sequence for predicting adduct formation.

Restriction Enzyme Analysis of Heat-Induced Double-Strand CC-1065 Lesions in SV40 DNA. The DNA polymerase termination assay data provided detailed information on the position of actual CC-1065 adduction sites in discrete regions of the genome. It was of interest to determine the

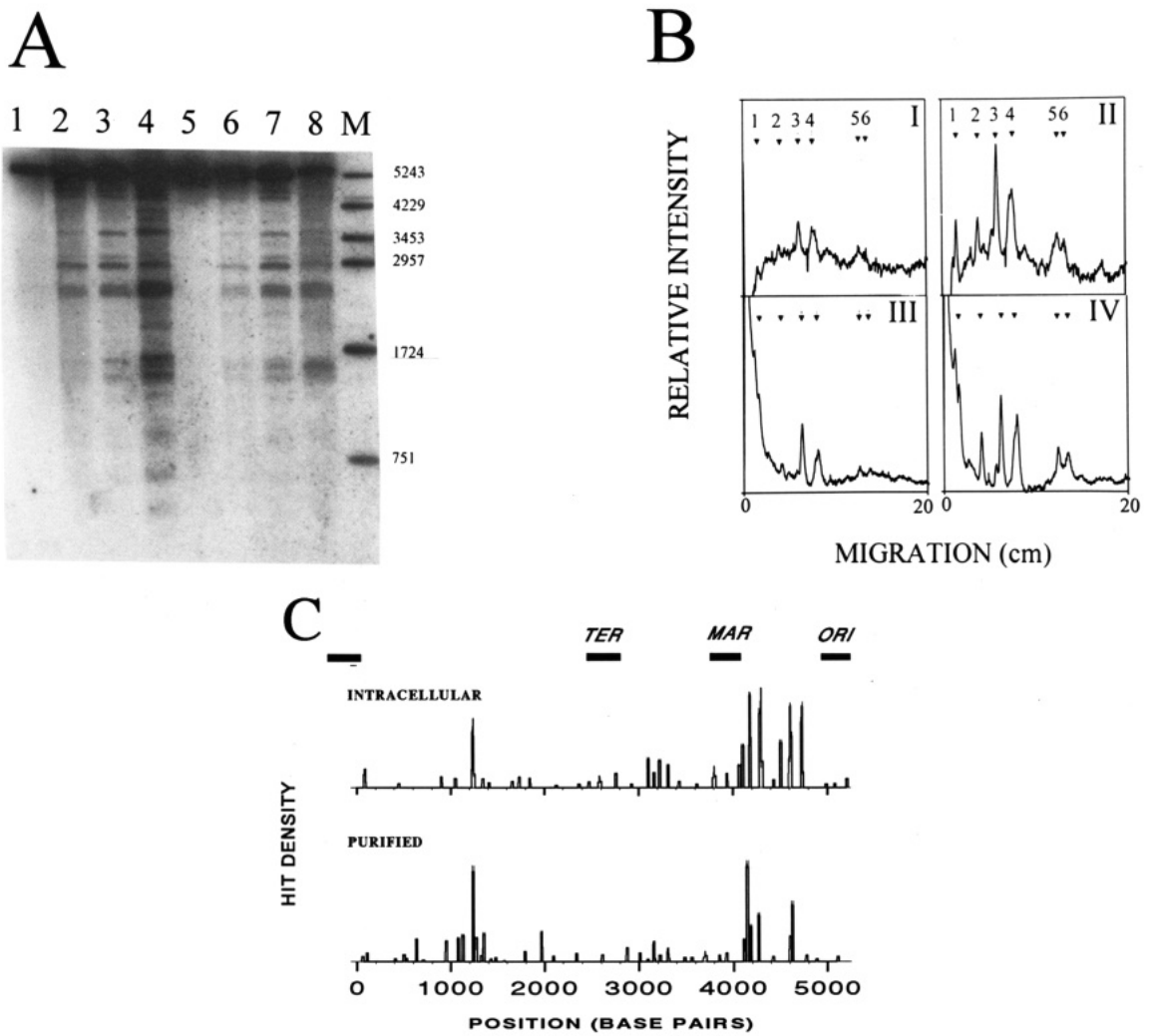

FIGURE 5: Double-strand SV40 DNA lesions induced by CC-1065: Restriction Enzyme Analysis. Restriction enzyme analysis was performed as described in Experimental Procedures. Panel A: Autoradiogram of representative blot showing electrophoresis of *Eco*RI-restricted CC-1065-treated samples hybridized to the *Eco*RI–*Bam*HI fragment of SV40. Lanes 1–4 show purified SV40 DNA treated with CC-1065 at r values of (1) 0, (2) 0.015, (3) 0.03, and (4) 0.15 (0, 50, 100, and 500 nM, respectively). Lanes 5–8 represent intracellular SV40 DNA treated with CC-1065 at r values of (5) 0, (6) 0.027, (7) 0.109, and (8) 0.546 (0, 0.5, 2, and 10 μM, respectively). M is an SV40 DNA size marker. Panel B: Densitometric scan of four lanes from the autoradiogram in panel A. Graphs I and II: intracellular SV40 treated with CC-1065 at r = 0.027 and 0.109, respectively. Graphs III and IV: purified SV40 DNA treated with CC-1065 at r = 0.015 and 0.03, respectively. The arrows indicate the position of double-strand breaks at about (1) 1000, (2) 60, (3) 4600, (4) 4200, (5) 3200, and (6) 3100 base pairs on the SV40 genomic map. Panel C: Apparent double-strand breaks induced by CC-1065 on intracellular and purified SV40 DNA over the entire genome. Break sites were determined from peak positions on the autoradiograms, while the relative density of any one band was calculated as a fraction of the density of all the DNA bands in a particular lane. The relative intensity thus obtained from analysis of each of the four enzyme restrictions at any one concentration of CC-1065 was summed to provide the "hit density". Each data point resulted from at least three separate experiments. Data were smoothed as described in Experimental Procedures. Regions of the genome (ORI, TER, and MAR) are as described in Figure 3.

location of these binding sites in the genome as a whole. A direct, albeit somewhat less precise, method of determining site preference of a DNA damaging agent is by restriction enzyme analysis. Strand breaks induced by heat treatment of CC-1065-treated DNA should be readily mapped by determining the size of the resultant fragments after electrophoresis of restricted samples. To this end, either intracellular or purified SV40 DNA was treated with CC-1065, at drug levels which were shown in Figure 2 to effect similar decreases in form I. Alkylated DNA was heated to induce strand breaks, digested with single-cut restriction enzymes, and subjected to agarose gel electrophoresis, Southern blotting, and hybridization to a ^{32}P-radiolabeled fragment of SV40 DNA as described in Experimental Procedures. Figure 5, panel A, is an autoradiogram of a representative agarose gel showing the effect of increasing concentrations of CC-1065 on the *Eco*RI restriction digestion pattern obtained with purified (lanes 1–4) and infected cell (lanes 5–8) SV40 DNA. The CC-1065 r values shown in this figure are identical to those in Figure 2, which produced similar changes in forms reduction when purified (r = 0.015–0.15) was compared to intracellular (r = 0.027–0.546) SV40 DNA treatment. A series of tight bands migrating faster than full-length linear SV40 (5243 base pairs) were observed in the drug-treated samples, suggesting several sites for neighboring damage on opposite strands in the SV40 molecule. In CC-1065-treated purified SV40 DNA samples, at least two bands were apparent at the lowest concentration shown (lane 2, r = 0.015). These bands persisted with increasing drug levels (r = 0.03 and 0.15; lanes 3 and 4, respectively), at which additional double-strand damage was detected. When damage to infected cells was examined, the electrophoretic pattern resembled that observed with purified DNA, albeit with higher r values (lanes 6–8; r = 0.027–0.546, respectively).

Figure 5, panel B, is a densitometric scan of selected lanes from the gel shown in panel A. Graphs I and II show heat-treated, *Eco*RI-restricted SV40 DNA from infected cells treated with CC-1065 at r = 0.027 and 0.109, respectively.

At the lower drug level (graph I), at least three regions can be detected with greater than background intensity. These regions show peak intensities at (3) 4600, (4) 4200, and (5) 3200 base pairs on the SV40 genome. At the higher drug concentration (graph II), at least two additional double-strand damage sites were observed with peak intensities at (1) 1000 and (2) 60 base pairs, while the region at 3200 resolved into two bands at (5) 3200 and (6) 3100. Although additional sites were apparent at the higher drug concentration, the major sites for DNA damage remained localized to regions around 4600, 4200, and 3200–3100. The peak intensities were in the order of 4600 ≥ 4200 > 3200 ≥ 3100. Similar profiles were found when purified SV40 DNA was treated with CC-1065 at $r = 0.015$ and 0.03 (graphs III and IV, respectively). At $r = 0.015$, two obvious peaks at 4600 and 4200 were observed, while at $r = 0.03$, additional sites were apparent in the regions 1000, 60, 3200, and 3100. The order of band intensity determined with *Eco*RI-restricted CC-1065-treated purified DNA was 4600 > 4200 > 3200 ≥ 3100.

To locate CC-1065 site preference damage over the entire SV40 genome, we utilized two SV40 fragments as hybridization probes and subjected CC-1065-treated DNA to restriction by a total of four single-cut restriction enzymes. A description of the method employed, as well as a summary of the heat-induced double-strand damage in CC-1065-adducted SV40 DNA, is shown in Figure 5, panel C. With both intracellular and purified SV40 DNA, double-strand break induction by CC-1065 was observed throughout the genome. Intracellular treatment with CC-1065 resulted in double-strand breaks concentrated in four distinct regions of the genome, with peak damage occurring in the region 4100–4300. The order of break intensity over these four regions was 4100–4300 > 4420–4750 > 1200–1300 > 3100–3300. Some minor damage also was detected in the origin region (5200–100). The pattern of break damage was similar, but not identical, when drug-treated purified DNA was analyzed. For example, damage to the region from 3100 to 3300 was relatively less pronounced in purified compared to intracellular DNA samples. Nevertheless, three major regions of DNA double-strand break intensity located at 4100–4300, 4400–4700, and 1100–1400 were identified in both purified and intracellular SV40 DNA samples.

When Figures 3, 4, and 5 were compared (regions of double-strand lesions determined by sequence analysis, DNA polymerase termination assay, and restriction enzyme digestion analysis, respectively), similarities in sites of double-strand lesions were immediately obvious. To better visualize where CC-1065 adduct formation and double-strand lesions occurred, a simplified map of the functional regions of the SV40 genome is shown in Figure 6. As would be expected, the restriction data revealed double-strand breaks in the same regions as the DNA termination assay. The region encompassed by 4410–4640 base pairs showed significant levels of double-strand adduct formation in all cases. This portion of the genome coincided with both the termination and the start of the coding regions for small and large T-antigens, respectively. Damage also was localized around 1100–1300, when cellular and purified DNA restriction studies were examined. Coding for the late viral protein genes has been localized to this area of the genome. Thus, regions of the SV40 genome capable of forming CC-1065 double-strand adducts can be predicted by examination of the known nucleotide base pair sequence of the preferred drug binding site.

Accumulation of SV40 DNA in CC-1065-Treated Virus-Infected Cells. One expected consequence of covalent adducts induced by CC-1065 in cellular DNA is the inhibition of

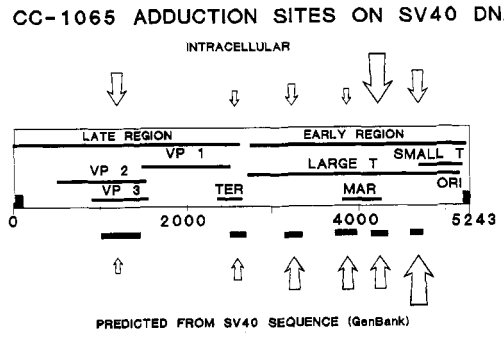

FIGURE 6: CC-1065 apparent double-strand lesion formation within the functional map of the SV40 DNA genome. Major sites predicted from the examination of the genomic sequence of SV40 described in Figure 3 are shown at the bottom of the figure, while intracellular sites determined by the restriction enzyme analysis described in Figure 5 are shown at the top. The size of the arrows reflects the density of adduct formation within the regions of the genome (indicated by heavy horizontal lines below the map) at 1000–1400, 2500–2700, 3100–3300, 3800–4000, 4100–4300 and 4500–4700 base pairs. VP1, VP2, and VP3 represent viral capsid proteins. Early and late regions refer to portions of the genome transcribed prior to and after initiation of viral DNA synthesis, respectively. TER, MAR, and ORI are as defined in Figure 3.

replication. Indeed, this drug was shown elsewhere to be a potent inhibitor of thymidine incorporation into cellular DNA (Li et al., 1982). Hence, it was of interest to examine whether the drug-induced damage to intracellular SV40 DNA was paralleled by an inhibition of viral SV40 replication. Drug effects on intracellular SV40 replication were first assessed by measuring total accumulation of viral DNA in infected cells. Cells were treated with CC-1065 at the onset of SV40 replication (2 h postinfection), when the amount of SV40 DNA was not detectable by ethidium bromide staining. Additional incubation until 40 h postinfection revealed the presence of viral DNA in control cells (Figure 7, panel A). Drug treatment caused a dose-dependent decrease in SV40 DNA accumulation. Quantitation of this effect (Figure 7, panel B) shows 50% inhibition at 2.5 nM, followed by the complete disappearance of SV40 DNA at 10 nM CC-1065. Similar inhibition of viral DNA synthesis was observed when virus was pretreated with CC-1065 prior to infection (data not shown).

CC-1065 Effects on Nascent SV40 DNA. The ability of CC-1065 to reduce replication of nascent SV40 DNA also was examined. In this system, SV40 replication intermediates were pulse-labeled with [^{14}C]thymidine after drug treatment. Consistent with previous studies (Snapka et al., 1988; Snapka & Permana, 1994), agarose gel electrophoresis of radiolabeled material from control cells revealed the presence of nascent SV40 DNA mainly in supercoiled form I, relaxed form II, and late Cairns intermediates (Figure 8, panel A). While SV40 infection resulted in a marked inhibition of cellular DNA synthesis, some residual incorporation into genomic DNA also was apparent. Incubation of infected cells with CC-1065 (1–200 nM) resulted in a concentration-dependent decrease in the amount of nascent material. Figure 8, panel B, is a graphic representation of the data in panel A. Based on the total loss of all viral DNA forms, a 50% inhibition of nascent DNA synthesis was observed at 60 nM CC-1065. Similar losses were observed when quantitation was done for each band separately (data not shown). Thus, drug action did not cause preferential accumulation of any of the replication intermediates. Though reduced, the formation of nascent form I continued in the presence of the drug, suggesting that DNA maturation is not unusually sensitive to CC-1065. In contrast to certain topoisomerase II inhibitors (Snapka &

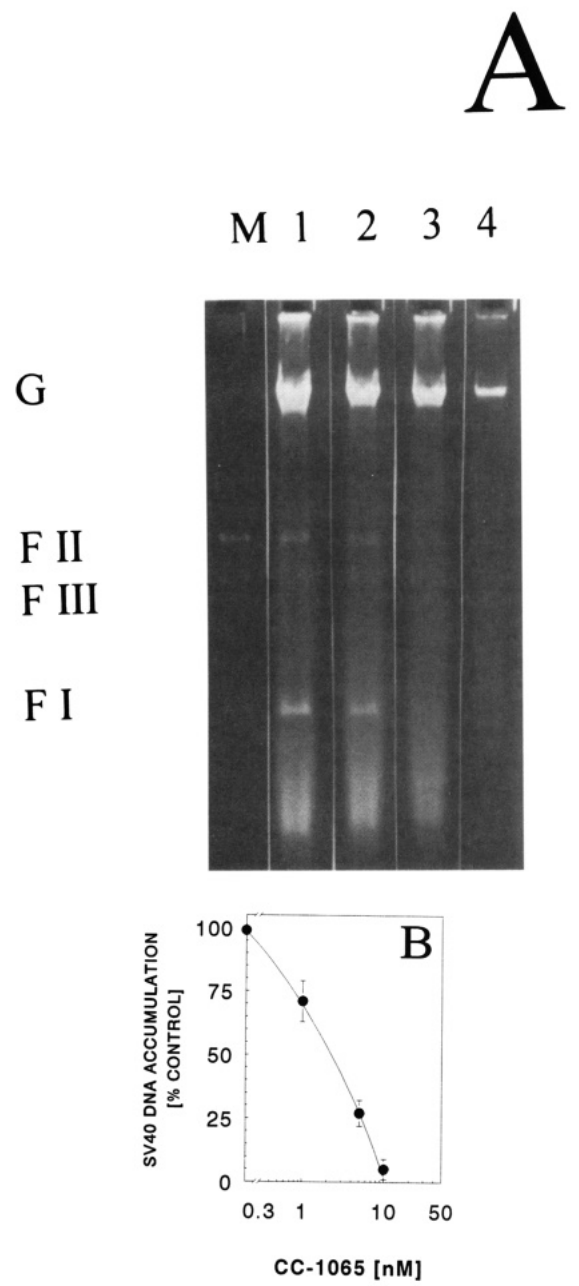

FIGURE 7: Inhibition of the accumulation of SV40 DNA in virus-infected BSC-1 cells. BSC-1 cells were infected with SV40 virus as described in Experimental Procedures. CC-1065 was added at the appropriate concentration 2 h postinfection. After 4 h, drug medium was replaced with fresh medium and incubation was continued for 36 h. Cells were lysed in SDS, digested with proteinase K, and analyzed for accumulation of SV40 DNA by agarose gel electrophoresis. Panel A shows a representative ethidium bromide-stained gel of SV40 DNA from infected cells treated with CC-1065. Lanes 1–4 represent drug treatment at (1) 0, (2) 1, (3) 5, and (4) 10 nM. Panel B shows the decrease in accumulation of SV40 DNA with increasing concentrations of CC-1065 observed in three experiments carried out in duplicate. Forms I and II were summed and the drug-treated samples were expressed as percent of control (0 drug) samples (±SEM). CC-1065 at 10 nM corresponds to $r = 0.003$.

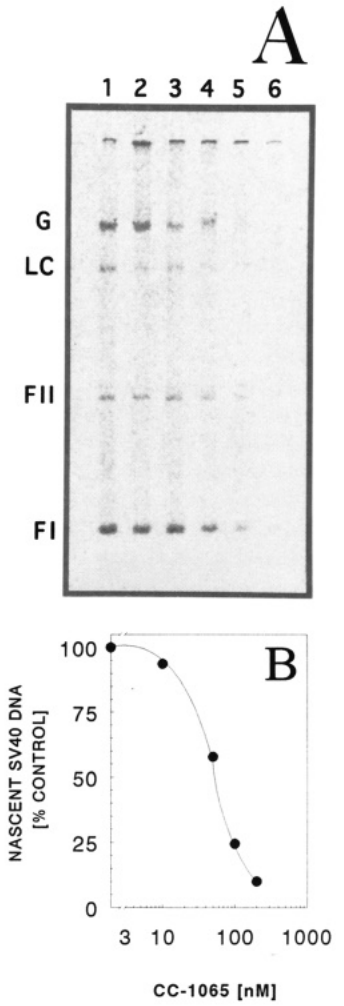

FIGURE 8: CC-1065 inhibition of nascent SV40 DNA synthesis in virus-infected BSC-1 cells. Cells were infected with SV40 as described in Experimental Procedures. CC-1065 was added 40 h postinfection and cells were further incubated for 4 h. At 44 h postinfection, [^{14}C]thymidine was added, and incubation was continued an additional 15 min. Replication intermediates were separated by agarose gel electrophoresis and visualized using a phosphorimager (panel A). Lanes 1–6 represent CC-1065 treatment at (1) 0, (2) 1, (3) 10, (4) 50, (5) 100, and (6) 200 nM. G, genomic DNA; LC, late Cairns structures; panel B shows the data from panel A. All the replication intermediates were summed and the drug-treated samples were expressed as percentage of control. CC-1065 at 100 nM corresponds to $r = 0.013$.

Permana, 1994), CC-1065 did not induce the formation of abnormal replication intermediates.

DISCUSSION

The present study marks the first time that the precise sites of CC-1065 lesions have been identified at the level of eukaryotic genomic DNA. Most of the previous studies examining CC-1065 DNA reactivity were performed on purified DNA fragments. While these studies provided essential information on base sequence preference and bond formation, little was known about how the drug interacted with its ultimate target, cellular DNA. In the eukaryotic cell, the bulk of DNA is packaged into nucleosome structures with which are associated various histone and non-histone proteins. Accessibility of cellular DNA to the action of CC-1065 might be limited by factors such as cell and nuclear compartmentalization or the protein components of cellular chromatin. Any of these factors, as well as the topological characteristics of larger size genomic DNA, might be expected to interfere with the base sequence preference of alkylation by CC-1065.

SV40 DNA provided a useful system for quantitating the effect of genomic DNA and chromatin components on CC-1065 adduct formation. The extent, as well as the position, of thermally induced CC-1065 lesions could be correlated with functional regions of the SV40 genome both in the absence and in the presence of chromatin structures (purified and infected cell SV40 DNA, respectively). Other workers previously examined CC-1065 binding in chromatin preparations from mouse P388 cells (Moy et al., 1989). Interestingly,

these workers found that most of the CC-1065 bound noncovalently to chromatin and that the majority (70%) of drug could be removed by phenol extraction. By contrast, they found CC-1065 binding to DNA was primarily covalent. This paper reports the extensive formation of irreversibly bound covalent adducts (CC-1065 which remains after phenol extraction) both in the absence and in the presence of chromatin proteins (purified and intracellular SV40 DNA, respectively). A possible reason for this discrepancy might reside in the differences in the two systems studied. P388 is a murine leukemia line maintained in continuous culture, and chromatin was isolated from these cells prior to drug treatment. By contrast, the BSC-1 line originated from monkey kidney cells, and chromatin studies were carried out in SV40 lytically infected cultures. Intracellular chromatin in lytically infected cells may provide a somewhat different target than isolated chromatin preparations. Additionally, chromatin accessibility may differ in chromatin originating from different species or target tissues.

Examination of the forms conversion data indicated that the presence of chromatin had little effect on the type of damage produced by covalently bound CC-1065. Though higher r levels of drug were required in the cellular assay, single-strand and apparent double-strand breaks accumulated in a similar fashion regardless of whether purified DNA or intracellular DNA was used as the drug target. These results are similar to SV40 damage induced by auromomycin, a protein antibiotic also isolated from a *Streptomyces* strain (Grimwade & Beerman, 1986). This drug interacts with DNA and causes both single- and double-strand breaks. As with CC-1065, when auromomycin was reacted with SV40 DNA, damage assayed in infected cells required 2–3-fold more drug than did purified DNA to achieve the same level of damage. Otherwise, accumulation of strand damage was the same regardless of the source of the DNA. Uptake parameters are among the possible reasons for the reduced efficiency of CC-1065 adduct formation in infected cells.

Increases in form II with increasing levels of CC-1065 were expected as a result of thermal induction of single-strand breaks at the site of the CC-1065 adduct. What was not expected was the extensive conversion to form III (indicative of double-strand damage) that was observed, even at low drug levels. Double-strand damage would be predicted to result from the location of sites of the appropriate binding sequence in close proximity on opposite strands. Such damage at low drug levels suggested a clustering of highly reactive bonding sites for CC-1065. Restriction analysis of thermally induced CC-1065 lesions in infected cells and purified SV40 DNA preparations revealed that, with the exception of an area of intense lesion formation at 1100–1300 base pairs, most of the high-affinity sites were localized to less than half of the genome (2500–5000 base pairs). These regions of observed double-strand adduct formation were predicted from analysis of the SV40 genomic sequence and reflected a high proportion of A-T base pair sequences. Runs of A-T base pairs have been associated with enhanced transcription (Bode et al., 1992; Pauly et al., 1992). The portion of the SV40 genome encompassed by 2600–5243 base pairs is termed the early region and is composed of sequences transcribed shortly after viral infection (i.e., large and small T-antigens).

Studies of analogs of CC-1065 have shown the importance of both the covalent and noncovalent binding components on drug activity (Sun et al., 1993; Boger et al., 1992; Hurley et al., 1988; Krueger et al., 1991; Krueger & Prairie, 1992). Covalent DNA bonding, however, is directly related to the cytotoxic potency of CC-1065 (Reynolds et al., 1986; Hurley et al., 1988; Zsido et al., 1991), and this agent has been shown to selectively inhibit DNA synthesis (Krueger & Prairie, 1992). The formation of highly localized lesions on SV40 DNA suggested that CC-1065 might severely impede the function of SV40 DNA. Indeed, a potent inhibition of viral replication based on a reduction in total SV40 DNA, as well as reduced thymidine incorporation into viral DNA, was observed with CC-1065 treatment of SV40-infected cells. The calculation of adduct frequency based on the forms conversion data in Figure 2 suggested that one adduct per SV40 molecule may be sufficient to prevent viral replication. Comparison of r values indicated that the effects on SV40 replication were detected at drug levels lower than those needed for adduct detection. Thus, it was possible that the lesions responsible for replication inhibition were even more specific than the detected adduct pattern. Such a suggestion is consistent with the differences in CPI bonding sites at various r values that have been observed by other laboratories (Boger et al., 1990a; Sun et al., 1993).

Obviously, an adduct anywhere in the genome may block the progress of the replication fork as observed with isolated polymerases (Li et al., 1982; also, see Figure 4, DNA polymerase termination assay). Since, in the DNA termination assay, we observed that *in vitro* DNA polymerization terminated at sites adjacent to adduct formation, inhibition of intracellular viral replication also might occur simply by blocking the movement of the replication fork. Interestingly, the level of adduct formation occurring was too low to account for the degree of replication inhibition observed. Additionally, our data indicated that CC-1065 did not prevent maturation of nascent SV40 DNA. Likewise, we found that the maturation of nascent genomic DNA in BSC-1 cells was not prevented by CC-1065 under conditions where the formation of nascent strands was severely inhibited (Woynarowski et al., unpublished data).

CC-1065 inhibition of intracellular formation of nascent viral strands may result from alterations in the synthesis of the early viral proteins produced prior to initiation of SV40 synthesis. Interestingly, many of the apparent intracellular double-strand adduction sites (see Figure 5C) were located within the coding region for large T-antigen, which is essential for initiation of SV40 viral DNA synthesis (Tooze, 1980). The transcriptional and replicative functions of DNA have been correlated with the ability of the helix to unwind, resulting, in some instances, in single-strandedness (Bode et al., 1992). CC-1065 alkylation and stabilization of the helix within the early region might prevent efficient transcription of the early genes.

In SV40, complexes of large T-antigen and replicating minichromosomes reportedly are attached to the nuclear matrix (Schirmbeck & Deppert, 1991), an important site of DNA replication and transcription [for reviews, see Fernandes and Catapano (1991)]. In SV40 DNA, matrix-associated regions (MAR) reportedly are responsible for the attachment of DNA loops to the nuclear matrix. The SV40 MAR also is notable for its association with high levels of topoisomerase II (Capranico et al., 1990; Pommier et al., 1990, 1991), which presumably function to separate daughter molecules after replication. Binding and cleavage by topoisomerase II in the absence of drug inhibitors has been observed primarily in the MAR region between 4100 and 4400 base pairs, within clusters of A-T base pairs. Since a large number of CC-1065-induced apparent intracellular double-strand lesions also were located between 4100 and 4300 base pairs, interference with the essential replicative functions of topoisomerase II might be an additional mechanism for DNA replication inhibition in

infected cells. Interestingly, other minor-groove binders have been shown to interfere with topoisomerase activity. This laboratory was the first to report that three such agents (distamycin, DAPI, and Hoechst 33258) were potent inhibitors of topoisomerase I and II, both in intact cells and in purified enzyme preparations (Woynarowski et al., 1988, 1989a,b; McHugh et al., 1989, 1990). CC-1065 also is capable of inhibiting the *in vitro* decatenation of *Crithidia fasciculata* DNA by purified preparations of topoisomerase II (Beerman et al., unpublished data). This inhibition may reflect the strong affinity of both CC-1065 and topoisomerase II for binding to A-T-rich regions as well as localization of their binding sites within the MAR region of SV40.

In conclusion, examination of SV40 DNA revealed that discrete regions of the genome contained a large proportion of the 5-base-pair A-T-rich CC-1065 consensus binding sequence. Very similar regions of intense bonding were obtained both by sequence analysis and by localization of actual intracellular adducts. This suggests that *in vitro* analyses using purified DNA are reflective of the intracellular DNA reactivity of CC-1065. Additionally, CC-1065 adduct formation in the SV40 genome results in a potent inhibition of intracellular viral DNA synthesis.

REFERENCES

Bhuyan, B. K., Newell, K. A., Crampton, S. L., & Von Hoff, D. D. (1982) *Cancer Res. 42*, 4542–4547.

Bode, J., Kohwi, Y., Dickinson, L., Joh, T., Klehr, D., Mielke, C., & Kohwi-Shigematsu, T. (1992) *Science 255*, 195–197.

Boger, D. L., & Sakya, S. M. (1992) *J. Org. Chem. 57*, 1277–1284.

Boger, D. L., Invergo, B. J., Coleman, R. S., Zarrinmayeh, H., Kitos, P. A., Thompson, S. C., Leong, T., & McLaughlin, L. W. (1990a) *Chem.-Biol. Interact. 74*, 29–52.

Boger, D. L., Coleman, R. S., Invergo, B. J., Sakya, S. M., Ishizaki, T., Munk, S. A., Zarrinmayeh, H., Kitos, P. A., & Thompson, S. C. (1990b) *J. Am. Chem. Soc. 112*, 4624–4642, 1990.

Boger, D. L., Munk, S. A., Zarrinmayeh, H., Ishizaki, T., Haught, J., & Bina, M. (1991a) *Tetrahedron 47*, 2661–2682.

Boger, D. L., Zarrinmayeh, H., Munk, S. A., Kitos, P. A., & Suntornwat, O. (1991b) *Proc. Natl. Acad. Sci. U.S.A. 88*, 1441–1445.

Borowiec, J. A., Dean, F. B., Bullock, P. A., & Hurwitz, J. (1990) *Cell 60*, 181–184.

Capranico, G., Jaxel, C., Roberge, M., Kohn, K. W., & Pommier, Y. (1990) *Nucleic Acids Res. 18*, 4554–4559.

Fernandes, D. J., & Catapano, C. V. (1991) *Cancer Cells 4*, 144–140.

Freifelder, D. (1969) *Biopolymers 7*, 681–694.

Grimwade, J., & Beerman, T. A. (1986) *Mol. Pharmacol. 40*, 458–464.

Grimwade, J., Cason, E. B., & Beerman, T. A. (1987) *Nucleic Acids Res. 15*, 6415–6429.

Hanka, L. J., Dietz, A., Gerpheide, S. A., Kuentzel, S. L., & Martin, D. G. (1978) *J. Antibiot. (Tokyo) 41*, 1211–1217.

Hurley, L. H., Needham-Van Devanter, D. R., & Lee, C.-S. (1987) *Proc. Natl. Acad. Sci. U.S.A. 84*, 6412–6416.

Hurley, L. H., Lee, C.-S., McGovren, J. P., Warpehoski, M. A., Mitchell, M. A., Kelly, R. C., & Aristoff, P. A. (1988) *Biochemistry 27*, 4886–4892.

Hurley, L. H., Warpehoski, M. A., Lee, C.-S., McGovren, J. P., Scahill, T. A., Kelly, R. C., Mitchell, M. A., Wicnienski, N. A., Gebhard, I., Jihnson, P. D., & Bradford, V. S. (1990) *J. Am. Chem. Soc. 112*, 4644–4649.

Krueger, W. C., & Prairie, M. D. (1992) *Chem.-Biol. Interact. 82*, 41–46.

Krueger, W. C., Hatzenbuhler, N. T., Prairie, M. D., & Shea, M. H. (1991) *Chem.-Biol. Interact. 79*, 265–286.

Lee, C. S., Sun, D., Kizu, R., & Hurley, L. H. (1991) *Chem. Res. Toxicol. 4*, 204–214.

Li, L. H., Swenson, D. H., Schpok, S. L., Kuentzel, S. L., Dayton, B. D., & Krueger, W. C. (1982) *Cancer Res. 42*, 999–1004.

Li, L. H., Kelly, R. C., Warpehoski, M. A., McGovren, J. P., Gebhard, I., & DeKonong, T. F. (1991) *Invest. New Drugs 9*, 147–148.

Lin, C. H., Hill, G. C., & Hurley, L. H. (1992) *Chem. Res. Toxicol. 5*, 167–182.

McGovren, J. P., Clarke, G. L., Pratt, E. A., & DeKoning, T. F. (1984) *J. Antibiot. 47*, 64–70.

McHugh, M. M., Woynarowski, J. M., Sigmund, R. D., & Beerman, T. A. (1989) *Biochem. Pharmacol. 48*, 2424–2428.

McHugh, M. M., Sigmund, R. D., & Beerman, T. A. (1990) *Biochem. Pharmacol. 49*, 707–714.

Moy, B. C., Prairie, M. D., Krueger, W. C., & Bhuyan, B. K. (1989) *Cancer Res. 49*, 1984–1988.

Neidle, S., Pearl, L. H., & Shelly, J. V. (1987) *Biochem. J. 244*, 1–14.

Pauly, M., Treger, M., Westhof, E., & Chambon, P. (1992) *Nucleic Acids Res. 20*, 975–982.

Petzold, G. L., Krueger, W. C., Swenson, D. H., Wallace, T. L., Prairie, M. D., & Li, L. H. (1985) *Proc. Am. Assoc. Cancer Res. 26*, 225.

Pjura, P. E., Grzeskowiak, K., & Dickerson, R. E. (1987) *J. Mol. Biol. 197*, 257–271.

Pommier, Y., Cockerill, P. N., Kohn, K. W., & Garrard, W. T. (1990) *J. Virol. 64*, 419–424.

Pommier, Y., Capranico, G., Orr, A., & Kohn, K. W. (1991) *J. Mol. Biol. 222*, 909–924.

Reynolds, V. L., Molineux, I. J., Kaplan, D. J., Swenson, D. H., & Hurley, L. H. (1985) *Biochemistry 24*, 6228–6247.

Reynolds, V. L., McGovren, J. P., & Hurley, L. H. (1986) *J. Antibiot. 49*, 419–444.

Sambrook, J., Fritsch, E. F., & Maniatis, T., (1989) *Molecular Cloning: A Laboratory Manual*, Cold Spring Harbor Laboratory, Cold Spring Harbor, NY.

Sanger, F., Nicklen, S., & Coulson, A. R. (1977) *Proc. Natl. Acad. Sci. U.S.A. 74*, 5463–5467.

Schirmbeck, R., & Deppert, W. (1991) *J. Virol. 65*, 2578–2588.

Snapka, R. M., & Permana, P. A. (1994) *BioEssays 15*, 121–127.

Snapka, R. M., Powelson, M. A., & Strayer, J. M. (1988) *Mol. Cell. Biol. 8*, 515–521.

Sun, D., & Hurley, L. H. (1993) *J. Am. Chem. Soc. 115*, 5925–5944.

Sun, D., Lin, C. H., & Hurley, L. H. (1993) *Biochemistry 32*, 4487–4495.

Tooze, J. (1980) *Molecular Biology of Tumor Viruses, Part 2*, Cold Spring Harbor Laboratory, Cold Spring Harbor, NY.

Warpehoski, M. A. (1986) *Tetrahedron Lett. 27*, 4104–4106.

Warpehoski, M. A., Harper, D. E., Mitchell, M. A., & Monroe, T. J. (1992) *Biochemistry 31*, 2502–2508.

Weiland, K. L., & Dooley, T. P. (1991) *Biochemistry 30*, 7559–7565.

Wierenga, W., Bhuyan, B. K., Kelly, R. C., Krueger, W. C., Li, L. H., McGovren, J. P., Swenson, D. H., & Warpehoski, M. A. (1986) *Adv. Enzyme Regul. 25*, 141–155.

Woynarowski, J. M., Sigmund, R. D., & Beerman, T. A. (1988) *Biochim. Biophys. Acta 950*, 21–29.

Woynarowski, J. M., McHugh, M., Sigmund, R. D., & Beerman, T. A. (1989a) *Mol. Pharmacol. 45*, 177–182.

Woynarowski, J. M., Sigmund, R. D., & Beerman, T. A. (1989b) *Biochemistry 28*, 4850–4855.

Zimmer, C., & Wahnert, U. (1986) *Prog. Biophys. Mol. Biol. 47*, 41–112.

Zsido, T. J., Woynarowski, J. M., Baker, R. M., Gawron, L. S., & Beerman, T. A. (1991) *Biochemistry 30*, 4744–4748.